

A HYBRID, BROADBAND, LOW NOISE CHARGE PREAMPLIFIER FOR SIMULTANEOUS  
HIGH RESOLUTION ENERGY AND TIME INFORMATION WITH LARGE CAPACITANCE  
SEMICONDUCTOR DETECTOR

M. GOYOT

Institut de Physique Nucléaire, Université Claude Bernard Lyon-1 and IN293,  
43, Bd du 11 novembre 1918, 69621 Villeurbanne, France

Summary

A broadband and low noise charge preamplifier was developed in hybrid form, for a recoil spectrometer requiring large capacitance semiconductor detectors. This new hybrid and low cost preamplifier permits good timing information without compromising energy resolution. With a 500 pF external input capacity, it provides two simultaneous outputs: (i) the faster, current sensitive, with a rise time of 9 nsec and 2 mV/MeV on 50  $\Omega$  load, (ii) the lower, charge sensitive, with an energy resolution of 14 keV (FWHM Si) using a RC-CR ungated filter of 2  $\mu$ sec and a FET input protection.

Introduction

Many circuits have been designed for the treatment of charges generated by semiconductor detectors<sup>1</sup>. For large capacitance ( $C_T = 500$  pF) thin detectors, the signal amplitude delivered by voltage amplifiers is very low. The energy resolution turns much too high. The current signal, which is proportional to the collecting time, is usually very short for this type of detectors. Therefore the timing information may be obtained either through a pick-off system or, directly after the current amplifier, through a constant fraction discriminator<sup>2</sup>. This timing information is also given either at the output of a charge preamplifier when the rise-time is very short<sup>3,4</sup> or after filtering by zero-crossing detection<sup>5</sup>. All these techniques produce very good experimental results but also show some disadvantages. The configuration which we propose, as well as that one described by Sherman<sup>6</sup>, allows one to obtain simultaneously timing and energy information. The faster of these, current sensitive, is a timing output. In this way, the delay time between the event and its detection is reduced to a minimum. This is of particular importance when an experiment of the recoil spectrometer type when multi-coincidences are needed between many different types of detectors. The slower

pulse is obtained from the output of the charge sensitive loop. Finally, the circuit is simple enough so as to make a hybrid design evolution possible.

Configuration of the preamplifier

The proposed configuration is presented on Figure 1. A fraction of the FET generated current is amplified by  $A_1$ . This current charges the feedback capacity  $C_f$  and gives the fast timing-signal. The voltage variation across  $C_f$ , read by the voltage amplifier  $A_v$ , provides the energy information. The response of the circuit to a short pulse of current  $I$  is as follows:

$$e_3(t) = -\frac{\alpha I}{C_f} e^{-\frac{\alpha}{R_f C_f} t} \quad (1)$$

for  $(A_1 + B_1) R_f g_m > \alpha$   
 $A_1$  and  $B_1$ : current gain in  $e_2$  and  $e_3$   
 $\alpha$ : voltage gain of  $A_v$

For a unit-gain ( $\alpha = 1$ ) one should consider the general case, presented on Figure 2. The total input capacity (detector, FET, paracitic) is represented by  $C_1$ . The output impedance in  $e_2$  may be assimilated to

$$Z_o(j\omega) = \frac{R_o}{1 + j\omega R_o C_o} \quad (2)$$

and the feedback impedance value is:

$$Z_f(j\omega) = \frac{R_f}{1 + j\omega R_f C_f} \quad (3)$$

If one takes  $A_1 g_m$  constant on the whole frequency band considered, it is possible to evaluate the variations of  $e_2$  and  $I_2$ . The voltages in  $e_1$  and  $e_2$  are equal to:

$$e_2(j\omega) = I(j\omega) \frac{(1 - A_1 g_m Z_f) Z_o}{j\omega C_1 (Z_o + Z_f) + 1 + A_1 g_m} \quad (4)$$

these values, for a FET slope of 50 mA/V is 10 ns. The contribution of the amplifier bandwidth increases when  $C_T$  decreases. Therefore one obtains better results with a simulation program of the IMAG2 type (Appendix). The whole circuit is shown on Figure 4. All the circuit parts are mounted on a 1" x 0.5" ceramic substrate and assembled in a 2 x 10 pin package (Figure 5).

### Performances

The equivalent noise charge (CEB) of the preamplifier depends directly on the FET noise sources<sup>8</sup> and on the detector characteristics. For high input capacities, one may consider that the CEB is equal to:

$$(CEB)^2 = \underbrace{\frac{e^2}{2} A_f C_T^2}_A + \underbrace{\frac{e^2}{2} \frac{KT}{\tau} \frac{0.7}{g_{m0}} C_T^2}_B + \underbrace{\frac{e^2 \tau}{4} \frac{1}{I_{inv}}}_{C} \quad (21)$$

where  $C_T$  is the total input capacity,  $I_{inv}$  the total leakage current,  $\tau$  the filtering time constant and  $A_f$  defines the noise in 1/f. The 1/f and white noise in series, A and B are represented on Figure 6 for the two types of tested transistors. Their contribution to the total noise is important. The mean measured values are respectively:

$$C413N \quad A_f = 1.6 \cdot 10^{-14} \text{ volt}^2, \quad g_{m0} \approx 55 \text{ mA/V}$$

$$2N4393 \quad A_f = 2 \cdot 10^{-14} \text{ volt}^2, \quad g_{m0} \approx 25 \text{ mA/V}$$

(2 FET mounted in parallel).

With  $A_f$  and  $g_{m0}$  one can make an estimation of the energy resolution in terms of the detector parameters. This evaluation is very close to the results obtained with a 800 nm<sup>2</sup>, 200 micron thick, RTC silicon detector (Figure 7). For an input capacity of 250 pF, the electronic contribution is 8.5 keV FWHM and for 500 pF it reaches 13.5 keV, for a RC-CR filtering of 2  $\mu$ sec. The maximum positive output signal is equivalent to 100 MeV referred to Si detector. The maximum negative signal level is about 25 MeV.

The noise current, at the input of the sensitive part of the current, measured on a frequency band of 10 MHz (RMS Fluke) is 50 nA for a total input capacity  $C_T$  of 500 pF. In fact, this corresponds to the noise generated by the channel resistance:

$$I_c = \left( \frac{4KT}{g_{m0}} \frac{0.7}{\tau} \right)^{1/2} C_T \approx \text{amp/Hz}^{1/2}$$

The amplitude and time responses are given in Figure 8, with  $C_T = 2.2$  pF. To this end, the current is injected by a low internal impedance tension generator, with a test capacity equivalent to the total input capacitance  $C_T$ .

The injection time being very short, the output amplitude as well as the rise-time depend directly on the bandwidth of the amplifier and on the circuit parameters (Equation 17).

The output pulses, current and charge sensitive, are shown on Figure 9, for a charge injection equivalent to 6.5 MeV, Si, using 500 pF external input capacitance. Figure 10 shows the same outputs obtained with the already mentioned detector and a thoron  $\alpha$  source (6.06 - 8.78 MeV). This allows one to appreciate the contribution of its undepleted zone resistance.

### Conclusion

The performances of the described circuit easily show that significant improvement is possible, in timing and energy resolution, with low cost hybrid circuit design.

### Acknowledgements

Many useful discussions with L. Vidal, M. Chevallier, J.P. Martin and B. Ilie are gratefully acknowledged.

### Appendix

The device models for circuit analysis programs are shown on Figure 11. With the steady-state operating conditions of current and voltage, the small signal transistor circuit model parameters were determined as follows:

$$r_e(\alpha) = 27/I_e \text{ (mA)}, \quad g_m = \frac{\beta}{(\beta+1)r_e}, \quad g_b'e = \frac{1}{r_e(\beta+1)}$$

$$\text{and } C_b'e = (1/w_T r_e) + C_{ib}$$

$r_{bb'}$  can be determined from the expression of noise figure or by measuring  $h_{11e}$  at a relatively high current and frequency, i.e.,

$$h_{11e} \approx r_{bb'} + r_e w_T / w$$

The field effect transistor parameters are given by the manufacturer's data sheets. The circuit of Figure 4 was analyzed using simulation program IMAG2. The parasitic inductance and capacitance associated to the components we used were introduced into the program description circuit. The plot of Figure 12 shows the output transient response predicted for a 1 MeV equivalent charge electronic injection by means of a 1 pF capacitor. Good agreement is obtained between the predicted and experimental results.

	$J_2$		$e_2$	
	$\theta > 3 \tau_m$	$\theta < \tau_m$	$\theta > 3 \tau_m$	$\theta < \tau_m/3$
Rise time	$2.2 \tau_m$	0	0	$2.2 \tau_m$
Max. amplitude	$I \left( \frac{C_f + C_0}{C_f} \right)$	$I \left( \frac{C_f + C_0}{C_f} \right) (1 - e^{-\theta/\tau_m})$	$\theta I / C_f$	

Table 1

## REFERENCES

1. A. Alberigi Quaranta, M. Martini, G. Ottaviani, IEEE Trans. Nucl. Sci., NS-15 (3), 35, 1968
2. J. K. Millard, T. V. Blalock, N. W. Hill, IEEE Trans. Nucl. Sci., NS-19 (1), 388, 1972
3. T. V. Blalock, IEEE Trans. Nucl. Sci., NS-13 (1), 457, 1966
4. M. Goyot, J. J. Samueli, A. Sarazin, N. I. M., 45, 149, 1967
5. W. J. McDonald, D. A. Gedcke, Intern. Symp. Nuclear Electronics, Versailles, tome I, 56, sept. 1968
6. I. S. Sherman, R. G. Roddick, IEEE Trans. Nucl. Sci., NS-17 (1), 252, 1970
7. V. Radeka, Nucleonics, 23, 52, July 1965
8. V. Radeka, Report BNL-12798, (1968), Brookhaven National Labs.

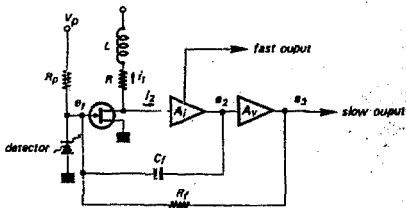


Figure 1 - Basic preamplifier stage

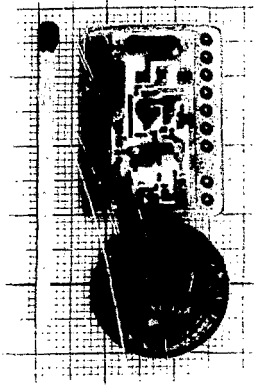


Figure 5 - Hybrid circuit photography

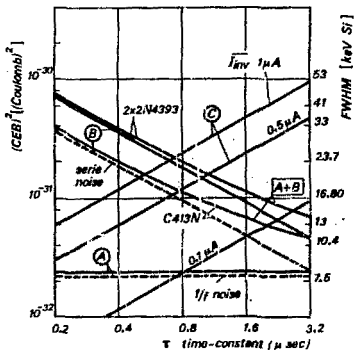


Figure 6 - Noise sources for two types FET with  $C_T = 500$  pF

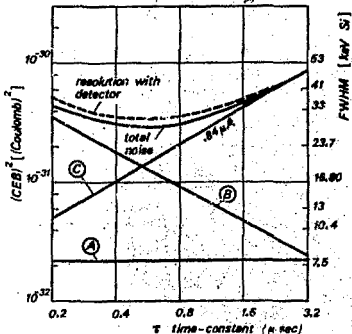


Figure 7 - Calculated total noise (A+B+C) and resolution obtained with RTC 102 detector (thoron a source)

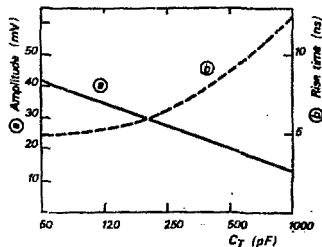


Figure 8

Plot of amplitude and time responses vs total input capacitance  $C_T$  (equivalent injection : 6 MeV Si).